

# Spatially resolved STIS spectra of WR+OB binaries with colliding winds<sup>1</sup>

Sébastien Lépine<sup>2</sup>, Debra Wallace<sup>3</sup>, Michael M. Shara<sup>2</sup>, Anthony F. J. Moffat<sup>4</sup>, & Virpi S. Niemela<sup>5,6</sup>

## ABSTRACT

We present spatially resolved spectra of the visual WR+OB massive binaries WR86, WR146, and WR147, obtained with the *Space Telescope Imaging Spectrograph* on board the *Hubble Space Telescope*. The systems are classified as follows: WR86 = WC7 + B0 III, WR146 = WC6 + O8 I-IIf, WR147 = WN8 + O5-7 I-II(f). Both WR146 and WR147 are known to have strong non-thermal radio emission arising in a wind-wind collision shock zone between the WR and OB components. We find that the spectra of their O companions show  $H_\alpha$  profiles in emission, indicative of large mass-loss rates, and consistent with the colliding-wind model. Our spectra indicate that the B component in WR86 has a low mass-loss rate, which possibly explains the fact that WR86, despite being a long period WR+OB binary, was not found to be a strong non-thermal radio emitter. Because of the small mass-loss rate of the B star component in WR86, the wind collision region must be closer to the B star and smaller in effective area, hence generating smaller amounts of non-thermal radio emission. Absolute magnitudes for all the stars are estimated based on the spectral types of the components (based on the tables by Schmidt-Kaler for OB stars, and van der Hucht for WR stars), and compared with actual, observed magnitude differences. While the derived luminosities for the WC7 and B0 III stars in WR86 are consistent with the observed magnitude difference, we find a discrepancy of at least 1.5 magnitudes between the observed luminosities of the components in each of WR146 and WR147 and the absolute magnitudes expected from their spectral types. In both cases, it looks as though either the WR components are about 2 magnitudes too bright for

---

<sup>1</sup>Based on Observations with the NASA/ESA *Hubble Space Telescope*, obtained at the Space Telescope Science Institute, which is operated by the Association of Universities for Research in Astronomy (AURA), Inc., Under NASA contract NAS 5-26555.

<sup>2</sup>Department of Astrophysics, Division of Physical Sciences, American Museum of Natural History, Central Park West at 79th Street, New York, NY 10024, USA, lepine@amnh.org, mshara@amnh.org

<sup>3</sup>Department of Physics and Astronomy, Georgia State University, Atlanta, GA 30303, wallace@chara.gsu.edu

<sup>4</sup>Département de Physique, Université de Montréal, C.P. 6128 Succ. Centre-Ville, Montréal, QC, Canada, H3C 3J7, moffat@astro.umontreal.ca

<sup>5</sup>Facultad de Ciencias Astronómicas y Geofísicas, Universidad Nacional de La Plata, Paseo del Bosque s/n, 1900 La Plata, Argentina, virpi@fcaglp.unlp.edu.ar

<sup>6</sup>Member of Carrera del Investigador, CIC-BA, Argentina

their spectral types, or that the O components are about 2 magnitudes too faint. We discuss possible explanations for this apparent discrepancy.

*Subject headings:* stars: Wolf-Rayet — stars: early-type — stars: winds, outflows — binaries: visual

## 1. Introduction

OB stars (which as a group include stars of spectral type between O3 and B2) are the most massive main sequence objects. They are generally found in young clusters and associations, because their lifespans are too short to carry them far from their birthplaces. Consequently, they are often subjected to considerable interstellar absorption. Wolf-Rayet (WR) stars are believed to be the evolved counterparts of at least some OB stars, and mostly correspond to a phase where the massive star has lost all its external hydrogen envelope through stellar winds (Conti 1976). Wolf-Rayet stars generate intense stellar winds reaching rates of  $\dot{M} \gtrsim 10^{-5} M_{\odot} \text{ yr}^{-1}$  and terminal speeds  $v_{\infty} \gtrsim 10^3 \text{ km s}^{-1}$ . The Wolf-Rayet photosphere arises not from the hydrostatic surface but in the wind itself which, besides He lines, is dominated either by ions of Nitrogen (WN stars) or Carbon and Oxygen (WC stars). Hence the spectrum of a WR star is dominated by very broad lines of He and heavier elements.

Current estimates indicate that at least  $\sim 40\%$  of WR stars are in multiple systems (Moffat 1995). The presence of a companion can be suspected from a composite spectrum showing OB absorption lines or from the apparent “dilution” of the WR emission lines by extra continuum emission (Smith *et al.* 1996). Confirmation of multiplicity is usually based on radial velocity studies. Indirect confirmation can also be made by the detection of colliding wind effects (e.g. Tuthill *et al.* 1999, Williams 1999). A small number of OB companions in very long period ( $P > 50 \text{ yr}$ ) systems have also been found from speckle interferometry or direct imaging (Hartkopf *et al.* 1993, Williams *et al.* 1997, Niemela *et al.* 1998). These systems are particularly interesting because the absolute magnitude of the WR component can be directly inferred from that of its companion, assuming the two stars are at the same distance.

In the IR and radio regimes, WR stars are dominated by thermal, free-free emission from the dense, expanding envelope. However,  $\approx 40\%$  of WR stars have been observed to have a radio spectral energy distribution consistent with non-thermal emission associated with synchrotron radiation and high-energy phenomena. Eichler & Usov (1993) have demonstrated how non-thermal radio emission could arise from the collision between the outflows from two early-type stars in a binary system. As it turns out, binary systems are over-represented in the sample of non-thermal emitters, which prompted van der Hucht (1992) to suggest that all non-thermal WR emitters were actually in binary systems, with the wind collision being responsible for the non-thermal emission.

The colliding wind model has been strikingly confirmed by radio observations of two

non-thermal WR emitters (Williams *et al.* 1997, Dougherty *et al.* 1996), confirmed to be in binary systems with OB companions (Niemela *et al.* 1998). The non-thermal emission is found to be associated with a distinct region whose photocenter is located *on or close to the line joining the WR star and its OB companion*, the WR star itself being associated with a thermal source. However, not all WR+OB binaries are found to be non-thermal emitters. Dougherty & Williams (2000) have noted that WR+OB systems form two distinct groups, with most thermal emitters being in short period systems, while the non-thermal emitters are all in long period systems, with large component separation. Since the non-thermal emission arises locally, at the wind-wind collision front, one might expect to observe non-thermal radio emission only from widely separated WR+OB binaries, whose large collision fronts are expected to be located well outside the extended radio photosphere of the WR wind. In short period binaries, the collision front occurs much deeper in the wind of the WR star, in which case non-thermal radio emission is not expected to be observed as the collision front lies inside the WR radio photosphere.

More recently, the conjecture that all non-thermal emitters are colliding wind binaries has been put in doubt by Wallace *et al.* (2000), who have failed to identify companions for 8 WR stars with non-thermal radio emission, down to a mean projected separation of  $\approx 20$  AU. Since this scale is within the distance of the radio photosphere, either non-thermal radio emission in these stars arises farther out in the wind itself (possibly generated by intra-wind shocks), or non-thermal radio emission does arise in colliding winds but the radio photosphere is much smaller than predicted. If the latter hypothesis is correct though, all the apparently single non-thermal radio emitters should have companions on close orbits, and should have been identified as spectroscopic binaries. The single-star explanation remains to be confirmed.

The colliding wind model, however, is successful in explaining non-thermal emission in long-period WR+OB systems. But are all long-period systems non-thermal emitters? So far, there is one exception to the rule: the long period WR+OB system WR86. However, while WR86 is not strictly defined as a non-thermal emitter, its spectral index is consistent with a “composite” thermal/non-thermal source, i.e. it is consistent with weak non-thermal emission (Dougherty & Williams 2000).

This paper presents spatially resolved STIS spectra of the components in the visual WR+OB systems WR86, WR146, and WR147. The observations and data reduction are discussed in Section 2. Spectral classification of the components is presented in Section 3. This allows us to estimate both the absolute luminosity of the components, and the mass-loss rates of the OB stars. Results are discussed in the light of the colliding wind model in Section 4. We briefly summarize our findings in Section 5.

## 2. Observations

Long-slit spectroscopy of the stars WR86, WR146, and WR147 have been obtained with the STIS spectrograph on board the *Hubble Space Telescope*. In each case, observations were carried out with the slit length oriented as close as possible to the apparent position angle of the binaries. Niemela *et al.* (1998) have estimated the position angles to be  $PA=109^\circ\pm 9^\circ$ ,  $21^\circ\pm 4^\circ$ , and  $350^\circ\pm 2^\circ$  for WR86, WR146, and WR147, respectively. The exact orientation of the STIS slit depends on the orientation of HST at the time of the observation; hence the above PAs were used as scheduling constraints. Observations were finally carried out with  $PA=106.1^\circ, 18.8^\circ$ , and  $360.2^\circ$ , for WR86, WR146, and WR147, respectively. In each case, the orientation was such that the brightest component in the V band appeared on the larger CCD column number. The width of the  $52\times 0.5$  arcsec slit is on the order of, or larger than, the separation between the components; hence the small difference ( $< 13^\circ$ ) between the orientation angle at the time of observation and the PAs of the systems has negligible effects on the throughput.

The two stars in the WR147 system are clearly resolved by STIS; we used standard IRAF aperture extraction to obtain their spectra. On the other hand, the relatively broad wings in the STIS point spread function (PSF) resulted in the WR86 and WR146 spectra being resolved, but with significant blending (Figure 1). To complicate matters, the shape of the PSF was found to be dependent on the wavelength, to a level that significantly affects the spectral extraction of barely resolved sources like those from WR86 and WR146 (but is however of little consequence for clearly resolved sources such as in WR147). We performed a multidimensional fit for each column on the CCD, to extract a blended double profile  $G(y)$  with the general shape <sup>7</sup>:

$$G(y) = A1 \exp -\left(\frac{(y - y1)^2}{2\sigma^2}\right)^k + A2 \exp -\left(\frac{(y - y2)^2}{2\sigma^2}\right)^k , \quad (1)$$

where  $y1$  and  $y2$  are the spatial locations of the stars along a column, and  $A1$  and  $A2$  are the amplitudes of the profiles for each star. The shape of the stellar profiles is governed by the dispersion parameter  $\sigma$  and the “peakyness” parameter  $k$  (which sets the relative strength of the PSF wings). Because the mean dispersion  $\sigma$  of the PSF is found to be close to the pixel size, we re-sampled the profile over individual pixels  $y_i$  from the continuous function  $G(y)$  using:

$$G'(y_i) = \int_{y_i-0.5}^{y_i+0.5} G(y)dy , \quad (2)$$

where  $y_i$  are integers representing the CCD lines.

We then used the assumption that the separation between the stars should be constant and independent of the wavelength. To determine the separation between the stars, we first performed

---

<sup>7</sup>The profile described by equation 1 is not a gaussian, although it does assume the gaussian form for the special case  $k = 2$ . We used this form for its simplicity and stability under the multi-dimensional fit. We did attempt to use other simple mathematical forms to describe the PSF, e.g. Moffat (1969) functions, only to obtain equivalent results in the spectral extraction.

a fit of  $G'(y_i)$  in the 6-dimensional parameter space  $(y_1, y_2, \sigma, k, A_1, A_2)$  and calculated the separation  $\Delta y$  between the stars from the mean values of  $y_2 - y_1$  obtained from each CCD column. We then fixed  $y_2 = y_1 + \Delta y$  and performed a second (more robust) fit in the 5-dimensional space  $(y_1, \sigma, k, A_1, A_2)$ , for each CCD column.

Using the derived values for  $\Delta y$  and the STIS pixel size of  $0.0507 \text{ arcsec pixel}^{-1}$ , we estimate the separation along the slit between the components of WR86, WR146 and WR147 to be  $0.239 \pm 0.006''$ ,  $0.161 \pm 0.005''$ , and  $0.624 \pm 0.015''$ , respectively. The PA of the slit was always within  $13^\circ$  of the line joining the two stars, hence these values should be reliable estimates of the component separations. Our values for WR146 and WR147 are consistent with the separation calculated from the WFPC2 image by Niemela *et al.* (1998). For WR86, our derived separation is outside of  $1\sigma$  of the  $0.286 \pm 0.039''$  range derived by Niemela *et al.*, but well within the  $0.230 \pm 0.013''$  range cited in the HIPPARCOS catalog.

Results of the multidimensional fits confirm the existence of a systematic variation in the PSF pattern with wavelength (Figure 2). The pattern also differs between WR86 and WR146, despite the same spectral coverage, which suggests that the shape of the PSF also depends on where the source falls along the slit (the WR86 and WR146 systems have been recorded on slightly different CCD columns). This raises the possibility that the PSF may be slightly different for each component in any one system, which may result in some inaccuracies in the spectral extraction.

The two stellar components in both WR86 and WR146 were apparently separated reasonably well across most of the spectral range. The only exception occurs at wavelengths close to the very bright WR emission line CIV  $\lambda 5808$  (at which point the WR star is significantly brighter than the OB star), where a small contamination of the WR flux onto the OB companion spectrum apparently occurred. This is clearly due to an imperfect PSF model. In particular, the wings of the PSF showed evidence for a weak diffraction pattern, which our model does not reproduce. This results in some contamination of one spectrum by some light from the other component. However, this contamination is apparent only for the broad CIV emission line, because of the large difference in the brightness of the WR and OB components at that wavelength, and is negligible elsewhere (below instrumental noise levels). Fortunately, this contaminated CIV emission from the WR component can be unambiguously identified in the OB star spectra, whose spectrum does not normally exhibit such a broad emission feature at that wavelength. Because the spectra are generally well separated, and because contamination effects are relatively small, we did not attempt to refine the PSF model further, which would have required the use of extra parameters and would have made the multi-dimensional fit much more difficult to perform.

The resolved spectra for all three stars are shown in Figure 3. It turns out that the brightest component in the V band in each pair is the Wolf-Rayet star, even though the continuum emission from the OB star is actually larger in WR86 and WR146 (the WR stars in these systems are brighter in V because of their strong emission lines). Contamination of the OB spectra by the very bright CIV  $\lambda 5812$  line is very obvious in WR146 (see Figure 5). Examination of the CIV

$\lambda 5812$  contamination profile in the spectrum of the O component shows that contamination becomes apparent as the monochromatic intensity from the WR star reaches  $\approx 3$  times that of the O companion. Since the relative WR intensity is below that level over the remainder of the spectrum, we conclude that contamination effects must be negligible over the remainder of the spectral range. Hence, any feature observed elsewhere in the spectrum of the O star is assumed to be intrinsic. In WR86, the components are further apart; hence the extracted spectra are less susceptible to contamination effects. Our extracted spectra of WR86 show evidence for a weak contamination of the CIV $\lambda 5812$  line, and also possibly from CIII  $\lambda 5696$  (see Figure 7). Both WR lines have monochromatic intensity reaching  $\approx 3$  times that of the B star continuum. Because these lines are the brightest features in the WR component of WR86, and because they yield only weak contamination effects, we conclude that no other WR features contaminate the B spectrum significantly, and any other feature observed in the B star spectrum must be intrinsic.

In each system, the slopes of the continua from the WR stars and the OB companions as well as the strength of the interstellar absorption lines are all consistent with equal amounts of reddening. This supports the idea that the components in each system are approximately at the same distance, and most likely to be physically related. In both WR146 and WR147, we confirm that the WR (O) component is to the south (north), consistent with the colliding wind interpretation of their radio maps (see Niemela *et al.* 1998). For WR86, the WR component is to the north-west and the B component to the south-east.

We did not find any trace of background, or “nebular” emission in the longslit spectral images, within the instrumental limits. Attempts have been made to extract spectra at different locations along the slit, but only the wings of the PSF from the stellar components and other instrumental features were detected. This lack of detection is significant for WR146 and WR147, which are known to be colliding wind binaries. If there is any diffuse emission in the optical associated with the colliding wind region, we estimate that it must be weaker than  $5 \times 10^{-15}$  ergs  $\text{cm}^{-2}$   $\text{s}^{-1}$   $\text{\AA}^{-1}$   $\text{arcsec}^{-1}$ .

Line identifications for each of the WR and OB star components are listed in Tables 1-6. The resolution of the STIS spectra was  $\approx 1.4\text{\AA}$ , which is the accuracy in the central wavelength measurements. Estimated errors on equivalent width measurements  $W_\lambda$  are listed individually. The error on  $W_\lambda$  depends on the strength of the line, and on whether it was resolved or in a blend. We do not give the mean central wavelengths of the lines in the WR stars, because the very broad profiles make the central wavelengths very unreliable for line identification. Most of the bright WR lines are actually blends of several different lines; the line identification and rest wavelength given in the tables is for the transition which most probably contributes to the largest part of the line emission.

### 3. Spectral Classification

### 3.1. WR86

This is the V=9th magnitude system HD156327, located at  $\alpha = 17\ 18\ 23.06$   $\delta = -34\ 24\ 30.6$  (J2000). It was initially listed as a Wolf-Rayet binary with spectral type WC7+B0 V (Roberts 1962; Smith 1968), based on the presence of H and HeI absorption lines in the blue. It was included in the Sixth Catalog of Galactic Wolf-Rayet stars (van der Hucht *et al.* 1981) under the designation WR86, and given a WC7+abs spectral type, implying that absorption lines could be intrinsic to the WR star, thus questioning its double star status. However, HD156327 was known to be a close visual double with separation  $\rho \sim 0.2''$  (Jeffers *et al.* 1963). The fact that Massey *et al.* (1981) failed to measure any radial velocity variation ruled out the idea of a *close* OB companion, strongly suggesting that the OB spectrum is associated with the visual companion (see Moffat *et al.* 1986). In any case, the star continued to be referred to as a WC7+abs throughout the 1980s.

The double star status was confirmed with speckle observations by Hartkopf *et al.* (1993), who resolved the star into two components with a  $0.237''$  separation. The components were also clearly resolved by the WFPC2 camera on board HST (Niemela *et al.* 1998). Based on scanned image tube spectra of the pair, Niemela *et al.* suggested the companion to be a B0 star (detection of OII, SiIII, and SiIV) with a luminosity class between I and III. The system is now listed in the seventh catalog of Wolf-Rayet stars (van der Hucht 2001) as “WC7 (+B0 III-I)”.

Our STIS spectra confirm that the WR component is of subtype WC7 (Figure 4, with line equivalent widths listed in Table 1). The ratio of the equivalent widths of the CIV  $\lambda 5801$  and CIII  $\lambda 5696$  lines is  $\log W_\lambda(\text{CIV } 5801)/\log W_\lambda(\text{CIII } 5696) \simeq 0.16$ , which is consistent with subtype WC7 in the quantitative classification system of Crowther *et al.* (1998).

For the O component (Figure 5; Table 2), our spectra confirm the B0 type, based on a comparison of the blue spectrum with the atlas of Walborn & Kirkpatrick (1990). We attempt to better constrain the luminosity class based on the strength of the  $H_\gamma$  absorption line, for which a calibration with the absolute magnitude has been derived by Millward & Walker (1985). We measure  $W(H_\gamma) = 2.60 \pm 0.15 \text{ \AA}$  the uncertainty being largely attributable to the blend with OII  $\lambda 4349$ . Following the Millward & Walker calibration, this corresponds to an absolute magnitude  $M_V \simeq -4.8 \pm 0.2$ . According to the B-star absolute magnitude calibration of Schmidt-Kaler (1982), this makes the star a B0 giant of class III. Since the WFPC2 photometry shows the two stars to have the same  $M_V$  (within the  $\pm 0.09$  observational errors), then the WR component is also estimated to have  $M_V \simeq -4.8 \pm 0.2$ . This value is largely consistent with the range of values quoted by van der Hucht (2001) for WC7 stars.

Luminosity classes of early B stars can also be estimated from the ratio of SiIII  $\lambda 5740$  and HeI  $\lambda 5876$ . Comparison with the yellow-red atlas of Walborn (1980) shows the spectrum to be generally consistent with luminosity class III. While we can definitely rule out a class I for this object, it is not possible to rule out spectral class II on the basis of the SiIII  $\lambda 5740$  / HeI  $\lambda 5876$  ratio. However, because the  $H_\alpha$  line shows no trace of overlying wind emission (which occurs in

most early B stars with luminosity class I-II), we classify this system as WC7 + B0 III.

### 3.2. WR146

This star, located at  $\alpha = 20\ 35\ 47.09$   $\delta = +41\ 22\ 44.7$  (J2000), was initially classified as WC6 by Roberts (1962), and as WC5 by Smith (1968). It was listed as a WC4 in the sixth catalog of Galactic Wolf-Rayet stars (van der Hucht *et al.* 1981). Improved measurements of the line ratios led Smith *et al.* (1990) to reclassify the WR star as WC6.

Dougherty *et al.* (1996) observed the star at 1.6 GHz and 2.5 GHz with the MERLIN array, and resolved the source into two components, a thermal source and a non-thermal source, separated by  $116 \pm 14$  milliarcseconds. They attributed the thermal source to the WR star, and the non-thermal source to a colliding-wind region between the WR star and an OB companion. Dougherty *et al.* (1996) also found weak hydrogen absorption lines ( $H_\delta$ ,  $H_\gamma$ ) in an unresolved blue spectrum of WR146, which they attributed to the unresolved companion.

Optical WFPC2 images from HST clearly resolved the object into two components separated by  $168 \pm 31$  arcsecs, and with very similar colors (Niemela *et al.* 1998). An overlap of the optical images and radio maps showed the non-thermal source to be located between the optical components, confirming the colliding-wind binary hypothesis. Assuming that the relative location of the non-thermal source matches the head of the bow shock, it is possible to calculate the ratio of the wind momentum fluxes. For WR146, Niemela *et al.* obtained a ratio  $\eta \equiv (\dot{M}v_\infty)_{OB}/(\dot{M}v_\infty)_{WR} \sim 0.1$ . Given the large mass-loss rate expected from the WC6 star, this requires the companion to have a relatively large mass-loss rate also. Based on the momentum ratio and on the relative colors of the components, Niemela *et al.* suggested the companion to be O6-O5 V-III.

More recently, Dougherty *et al.* (2000) obtained a 3800 – 4500Å spectrum of WR146 at the 4-m William Herschel Telescope (WHT). Though blended with emission lines from the WR star, the relatively narrow absorption lines from the O companion were clearly identified. Their  $\lambda 4541$  HeII /  $\lambda 4471$  HeI equivalent width ratio (the principal diagnostic of the O-type sequence) indicated a spectral type O8. Though several features were also suggestive of a high luminosity class, they did not assign a luminosity class due to a lack of the main luminosity diagnostic lines in their spectrum. The system is now listed as WC6+O8 in the seventh catalog of Wolf-Rayet stars (van der Hucht, 2001).

Our STIS spectra of the WR component (Figure 6; Table 3) confirms the WC6 classification. We measure a line equivalent width ratio  $\log W_\lambda(\text{CIV } 5801)/\log W_\lambda(\text{CIII } 5696) \simeq 1.03$ , consistent with subtype WC6 in the quantitative classification system of Crowther *et al.* (1998). The lines in this star are especially broad, indicating a large wind terminal velocity ( $v_\infty \simeq 2900$  km s<sup>-1</sup> as measured by Eenens & Williams 1994).



For the OB component (Figure 7; Table 4) we measure a line ratio He II  $\lambda 4541$  / He I  $\lambda 4471$  = 0.39 which is consistent with a spectral type O9 in the system of Conti & Alschuler (1971) and Conti (1973). The HeI  $\lambda 4471$  line does look significantly broader than HeII, which may be due to noise, but could also result from blending of the HeI  $\lambda 4471$  with some other unidentified line. On close examination, the HeI  $\lambda 4471$  profile in the B0 III component of WR86 does look asymmetric, with the blue side of the line being unusually extended. If this is due to some unidentified IS absorption feature (we do indeed see a shallow absorption trough at the same wavelength in the WR spectrum which could also be the signature of this IS feature, see Figure 6), then the EW of this line is most likely to be overestimated in WR146. We consider the HeI  $\lambda 4388$  line, and note that it is clearly weaker than HeII  $\lambda 4540$ ; the spectral atlas of Walborn & Fitzpatrick (1990) shows that this generally does not occur in O9 type stars, where both lines have about the same EW. It is however consistent with spectral type O8, and we thus also adopt this classification for the O star in WR146.

The main luminosity diagnostic for O8-O9 stars is the increase in the strength of the Si IV  $\lambda\lambda 4089, 4116$  at higher luminosities, and the change in NIII  $\lambda\lambda 4634, 4640$  and He II  $\lambda 4686$  from absorption to emission (Walborn & Fitzpatrick, 1990). While the WHT spectrum of Dougherty *et al.* included both Si IV lines, they were found to be blended with the  $H_\delta$  line. Unfortunately, neither the STIS nor the WHT spectrum covers the He II  $\lambda 4686$  region. However, we note the presence of a weak emission feature centered on  $\lambda 5696$  which we attribute to CIII line emission. Both the CIII  $\lambda 5696$  and  $H_\alpha$  lines have been shown by Walborn (1980) to behave like NIII  $\lambda\lambda 4634, 4640$  and He II  $\lambda 4686$ , respectively.

The  $H_\alpha$  profile in the O star component shows a narrow but relatively shallow absorption trough flanked by relatively broad wings. The  $H_\alpha$  line in the O star is coincident with the HeII  $\lambda 6560$  complex in the Wolf-Rayet star, which raises the possibility of contamination into the O spectrum, which would explain the broad wings. However, we argue that the broad  $H_\alpha$  emission profile is intrinsic to the O star: (1) the intensity of the HeII  $\lambda 6560$  complex relative to the O star continuum is comparable to that of the broad shoulder in the CIV  $\lambda 5812$  complex (between  $\lambda 5850$  and  $\lambda 5950$ ), and we see no obvious contamination of the O star spectrum by the latter, (2) the  $H_\alpha$  profile in the B0 component in WR86 does not show any broad wings, while it was more prone to being contaminated by the more intense HeII  $\lambda 6560$  complex from its WR component, (3) the centroid of the  $H_\alpha$  absorption trough is  $6.4\text{\AA}$  larger than the measured lab value, which suggests that the central trough is being distorted as the line is filled up with  $H_\alpha$  in emission, and (4) the overall shape of the  $H_\alpha$  profile is very similar to that of other OIf stars (e.g. Cygnus OB#7 and HD210839 see Figure 6 in Herrero *et al.* 2000), including both the central narrow absorption and the broad emission wings.

The behavior of CIII  $\lambda 5696$  and  $H_\alpha$  in the O component of WR146 clearly rules out any luminosity class fainter than II. Because the  $H_\alpha$  line is not found to be strongly in emission, as in O8 I stars, a spectral type O8 II is the most reasonable classification. A secondary indicator for the luminosity class is the ratio He I  $\lambda 4388$  / He I  $\lambda 4471$ , which correlates with the mass-loss

rate. Our spectrum yields  $\text{He I } \lambda 4388 / \text{He I } \lambda 4471 = 0.2$ , which suggests that the star is Of. The weakness of  $\text{H}_\gamma$  ( $W_\lambda = 1.5$ ) is also consistent with large intrinsic luminosity; the Millward & Walker (1985) relationship suggests  $M_V \gtrsim -6$  which, for O8, is consistent with luminosity class I-II (Schmidt-Kaler 1982). From these lines of evidence, we classify this system as WC6 + O8 I-III.

### 3.3. WR147

This star, located at  $\alpha = 20\ 36\ 43.65$   $\delta = +40\ 21\ 07.3$  (J2000), was resolved into a double radio source with a thermal lobe and a non-thermal lobe by Churchwell *et al.* (1992). Williams (1996) hypothesized that the non-thermal lobe was the result of a colliding-wind interaction with an unseen companion. The companion was first identified as a faint component in an IR image of WR147 (Williams *et al.* 1997), and confirmed in the optical by HST WFPC2 observations (Niemela *et al.* 1998). Based on the relative K magnitude between the WN8 star and the IR companion ( $K_{OB} - K_{WR} = 3.04 \pm 0.09$ ), and assuming the WN8 star to have an absolute magnitude  $M_K \approx -6$ , Williams *et al.* claimed the OB companion to be consistent with a spectral type B0.5 V. In the optical, the magnitude difference between the two components is observed to be  $V_{OB} - V_{WR} = 2.16 \pm 0.09$ , which is too small for a B0.5 V companion, and Niemela *et al.* (1998) proposed that the star is of earlier type.

Our STIS data for the WR component in WR147 (Fig. 8; Table 5) shows a spectrum typical of a WN8 star, with a relatively strong P Cygni profile in HeI  $\lambda 5876$ . Also present are the weak HeII  $\lambda\lambda 6311, 6406, \text{ and } 6527$  lines — all with P Cygni profiles. Weak NII  $\lambda\lambda 5680, 5686$  lines are also detected, consistent with a late-type WN star.

Our WR147 spectrum in the blue regime is of very poor quality and is not shown in this paper. Because of the considerable interstellar reddening, the WR147 system is several magnitudes fainter in the blue, and our HST STIS exposures were not programmed appropriately for this relatively faint target. Hence it is not possible to obtain a precise, reliable spectral type for the O component since classification of OB stars is largely based of the ratio of HeI and HeII lines in the blue. However, our spectrum shows a very weak HeI  $\lambda 5876$  line, while HeI  $\lambda 6678$  is too weak to even be detected (Fig.9; Table 6). Since HeI is very strong in late O stars and early B stars (type B2 being where HeI reaches a maximum; see Walborn & Fitzpatrick 1990), this suggests that this star is either earlier than O8, or mid/late B. Because He becomes doubly ionized in early O stars, we can also exclude a spectral type earlier than O5. Furthermore, the presence of high ionisation CIV lines unambiguously rules out any spectral type B or later. These lines of evidence suggests that our star can only be in the range O5-O7. An O5-O7 spectral type is consistent with the relatively strong CIV  $\lambda\lambda 5801, 5812$  lines, which are strongest in this spectral range (Walborn 1980). Because we lack a clear line ratio, and because there is considerable scatter among O stars in the equivalent widths of single species, it is however not possible to constrain the spectral type further. Due to the lack of other objective classification criteria, the O5-O7 assignment must be

regarded as tentative.

The  $H_\alpha$  region shows a very shallow absorption trough, flanked by broad emission wings, very similar to the profile observed in the O8 component in WR146. The broad emission wings cannot be explained by contamination from the WN8 star, since the two components are well resolved by STIS and any (very weak) component arising in the very broad wing of the STIS PSF from the WN8 star should be subtracted out with the background in the aperture extraction procedure. Furthermore, the centroid of the observed absorption trough is  $8.9\text{\AA}$  over the  $H_\alpha$  laboratory wavelength; this suggests that the line profile is significantly distorted as it is filled up with  $H_\alpha$  emission arising in the wind. Finally, the overall shape of the  $H_\alpha$  profile is very similar to that of other O If stars (e.g. Cygnus OB#7 and HD210839, Herrero *et al.* 2000).

This  $H_\alpha$  emission suggests a substantial mass loss rate, which would imply that the star is a supergiant in the Of category. However, CIII  $\lambda 5696$  is not clearly in emission; this is more consistent with stars in the (f) category, which show a filling in of HeII  $\lambda 4686$  but no strong emission lines. It is therefore not possible at this point to clearly distinguish between spectral class Ia, Iab, Ib, or II, but luminosity classes III-V can be excluded. We tentatively classify this star as O5-7 I-II(f).

## 4. Discussion

### 4.1. On the absolute magnitudes of the components

Absolute magnitudes  $M_v$  (in the narrowband photometric system defined by Westerlund 1966) have been estimated for Galactic WR stars on the basis of cluster and association membership (van der Hucht 2001, hereafter vdH01). The narrowband  $v$  is used because it avoids the brightest optical emission lines of WR stars. The distances of clusters and associations derived by L undstrom & Stenholm (1984) are used. The mean absolute magnitudes  $M_v$  for WC7, WC6, and WN8 stars are  $M_v \simeq -4.5$ ,  $-3.5$ , and  $-5.5$ , respectively, with a standard deviation  $\lesssim 1.0$  magnitude.

The absolute magnitudes  $M_V$  of the OB stars can be estimated, based on their spectral classification, using the relationships defined by Schmidt-Kaler (1982, hereafter SK82). While the  $v$  and  $V$  bands are not exactly the same, a comparison between  $V$  and  $v$  for a number of WR and OB stars shows that  $|v - V| \lesssim 0.3$  (Westerlund 1966, see also Turner 1982). While the value of  $v - V$  for any given WR star will be dependent on the strength of the optical lines, we can assume that  $M_v \sim M_V$  to within less than half a magnitude.

We thus compare the difference in absolute magnitudes as determined from the spectral types with the measured difference in  $V$  derived using the WFPC2 images of these systems by Niemela *et al.* (1988). For the WR86 system, the WC7 star is expected to be in the range  $-5.5 < M_V < -3.5$ , and SK82 quotes a value of  $M_V \simeq -5.1$  for a B0 III star. The two estimates are thus consistent with each other, since the observed difference in  $V$  magnitude for this system

is  $V_{WR} - V_B = 0.02 \pm 0.18$ .

For the WR146 system, the WC6 star is expected to be in the range  $-4.5 < M_V < -2.5$ , while SK82 quotes a mean value of  $M_V \simeq -6.25$  for O8 I-II stars. The observed magnitude difference is  $V_{WR} - V_B = -0.24 \pm 0.08$ ; there is thus a discrepancy of at least 2 magnitudes between the observed magnitude difference and that inferred from the spectral types. The two stars are definitely companions, as evidenced by the confirmation of a colliding wind region between the two components. The discrepancy thus cannot be attributed to a chance alignment of two stars at different distances. If we assume that the O8 star is actually a main sequence object (unlikely because of the  $H_\alpha$  line in emission), we get  $M_V = -5.15$  from SK82, which still yields a difference of at least one magnitude. This means either that the WR star is too bright for its spectral type or, alternately, that the O star is too faint. An intriguing comparison can be made between WR146 and WR86: both systems have components of approximately the same magnitude, but the WC5 star in WR146 is expected to be intrinsically fainter than the WC7 star in WR86, while the O8 I-II star in WR146 is expected to be intrinsically brighter than the B0 III star in WR86.

For the WR147 system, the WN8 star is expected to be in the range  $-6.5 < M_V < -4.5$ . From SK82, we get a range of values  $-5.90 < M_V < -6.25$  for O5-7 stars with luminosity classes I-III. The observed magnitude difference is  $V_{WR} - V_B = -2.16 \pm 0.12$ . Again, we find that the WR component is too bright for its spectral type by at least 1.5 magnitudes or, alternately, that the O star is too faint by at least 1.5 magnitude. To be consistent with the expected magnitude of a WN8 star, the O star would have to be fainter than  $M_V \approx -4.4$  which, in the SK82 tables, is only consistent with stars of type B0 or later. A spectral type of B is clearly ruled out by our STIS spectra.

Recently, absolute magnitudes of OB stars were re-evaluated, based on data by HIPPARCOS (Wegner 2000, hereafter W00). The values of  $M_V$  for giant and supergiant OB stars derived by W00 turn out to be fainter than the SK82 values by about 2 magnitudes. Under the W00 system, the absolute magnitudes of WR146 and WR147, as estimated from the spectral types would be consistent with the observed magnitudes. Although the agreement is suggestive, one has to be concerned about the possible effects of the revised  $M_V$  from the W00 system on the distance to Galactic clusters and associations, and hence on the absolute magnitudes derived by vdH01. One also has to consider the relatively large scatter in the absolute magnitudes of individual OB stars as derived from HIPPARCOS parallaxes. For O7-B0 stars, the scatter can be as large as  $\pm 1$  magnitude. There may also be systematic effects on parallax estimates of the OB star HIPPARCOS sample, especially since most of the OB stars are beyond 200pc. Hence, the values derived from W00 must be used with caution.

Some of the discrepancy may arise because of the uncertainty in the determination of the spectral-type of the OB components. In particular, the main criterion used in the determination of the luminosity class was the apparent filling in of the  $H_\alpha$  line, which suggests high mass-loss rates in WR146 and WR147. However, both WR146 and WR147 are systems with colliding winds. If

$H_\alpha$  emission arises in the shock front, this could fill-up the  $H_\alpha$  absorption line in the spectra of the OB companions, mimicking the effect of intense mass-loss. If  $H_\alpha$  emission arises near the head of the bow shock front, which is relatively close to the O star in both WR146 and WR147, then we would not be able to resolve them from the O star in the STIS data presented here, and this might explain the apparent filling in of the emission lines. On the other hand, if  $H_\alpha$  emission was to arise downwind from the head of the bow shock, at some relatively large distance from both the WR and O components, then any extra  $H_\alpha$  emission would appear as a diffuse component on the STIS data, which would not be strong enough (as we have shown from the lack of any detected diffuse emission, see section 2) to account for the apparent filling in of the emission lines.

#### 4.2. On the binary status and the wind collision

The WR146 and WR147 systems exhibit strong non-thermal radio components. It has been found that the non-thermal emission occurs *between* the two stellar components, somewhat closer to the OB star (Dougherty *et al.* 1996, Williams *et al.* 1997). In the framework of the colliding wind model developed by Eichler & Usov (1993), the shock front forms at a distance  $r_{OB}$  ( $r_{WR}$ ) from the OB (WR) component. Given  $D = r_{OB} + r_{WR}$  the distance between the two stars, then:

$$r_{OB} = \frac{\eta^{1/2}}{1 + \eta^{1/2}} D, \quad (3)$$

where  $\eta \equiv (\dot{M}v_\infty)_{OB}/(\dot{M}v_\infty)_{WR}$  is the wind momentum ratio. The ratio  $r_{OB}/D$  is dimensionless and independent of the projection of the system on the plane of the sky, and thus can be measured directly from imaging.

For WR146 and WR147,  $r_{OB}/D \simeq 0.25$  and  $0.14$ , respectively, as measured directly from the combined radio maps and HST WFPC2 images (Niemela *et al.* 1998). These yield estimated values of  $\eta = 0.10$  and  $\eta = 0.028$  for WR146 and WR147, respectively. From the spectral types, we estimate that the O components in WR146 and WR147 have mass-loss rates  $\dot{M}_O \sim 110^{-5} M_\odot \text{ yr}^{-1}$  (see Herrero *et al.* 2000). If we assume a typical terminal velocity  $v_\infty \approx 2000 \text{ km s}^{-1}$  for the O stars (see Prinja, Barlow & Howarth 1990), we can estimate the mass-loss rate of the WR components and check for consistency. For WR146, taking  $v_\infty = 2900 \text{ km s}^{-1}$  as the terminal velocity of the WC6 star, this yields a mass-loss rate  $\dot{M}_{WR} \sim 6.9 \cdot 10^{-5} M_\odot \text{ yr}^{-1}$ . This value is consistent with the mass loss rate value of  $\dot{M}_{WR} = 3.0 \pm 1.5 \cdot 10^{-5}$  derived from the radio emission of the WR star by Dougherty *et al.* (1996). For WR147, however, taking  $v_\infty = 1100 \text{ km s}^{-1}$  as the terminal velocity of the WN8 star (from Eenens & Williams 1994), one gets  $\dot{M}_{WR} \sim 6.5 \cdot 10^{-4} M_\odot \text{ yr}^{-1}$ , which is an order of magnitude larger than the mass-loss rate value of  $\dot{M}_{WR} = 4.6 \cdot 10^{-5}$  estimated from the radio emission by Williams *et al.* (1997).

For WR147, Williams *et al.* (1997) have deduced a distance of  $\approx 630 \text{ pc}$  by comparing infrared photometry of WR147 and WR105, the latter being another WN8 star suspected to be in the Sgr OB1 association, whose distance is known. It is from this estimated distance and from VLA

measurements of the radio flux that Williams *et al.* (1997) have estimated the mass-loss rate in the WR component of WR147 to be  $4.2 \pm 0.2 \cdot 10^{-5} M_{\odot} \text{ yr}^{-1}$ . The disagreement with our estimated value can be resolved in two ways: (1) we have overestimated  $\dot{M}_O$  by at least an order of magnitude, in which case the OB component in WR147 is unlikely to be an O supergiant, or (2) WR147 is more distant than estimated by Williams *et al.* (1997), i.e. at least 1 kpc away. If the latter interpretation is true, then there exist significant differences between the spectral energy distributions of WR105 and WR147. The former interpretation is more likely to be true, which means that we have overestimated the mass-loss rate of the O component because of an inaccurate assessment of the spectral type and luminosity class. The key element here is the observation of the filling in of the  $H_{\alpha}$  profile, which does suggest a high mass-loss rate and luminosity. Clearly, a resolved spectrum of the OB component in WR147 spanning the whole optical range is required to resolve this issue. Such an observation will have to be performed with the Hubble Space Telescope, or with similar high spatial resolution from the ground.

While WR86 does show evidence for some non-thermal emission, it is listed by Dougherty & Williams (2000) as having a “composite” spectral energy distribution (as compared to a “non-thermal” spectral energy distribution for WR146 and WR147, and a “thermal” energy distribution for suspected single WR stars). We believe that the fact that this star has only a weak component of non-thermal emission can be explained by the smaller mass-loss rate from the B component. While late Of stars typically have derived mass-loss rates  $\dot{M} \sim 10^{-5} M_{\odot} \text{ yr}^{-1}$ , a star of spectral type B0 III like the companion to WR86 is expected to have a mass-loss rate  $\sim 10^{-7} M_{\odot} \text{ yr}^{-1}$ , or about two orders of magnitude smaller than Of stars (e.g. Runacres & Blomme 1996). Assuming  $V_{\infty}$  for the B0 III star to be of the same order of magnitude as for the supergiant O stars in WR146 and WR147, this means that the wind momentum from the B0 III star must be two orders of magnitude smaller and  $r_{OB}$ , the distance from the OB star to the wind collision front, is expected to be one order of magnitude smaller for the WR86 system than it is for WR146 and WR147. This means that the WR86 shock front is formed much closer to the OB component and most likely wraps around the OB component with a much smaller opening angle. Hence, the total volume where non-thermal emission occurs should be significantly smaller, which accounts for the weaker non-thermal emission. This hypothesis can be tested by imaging the WR86 system in the IR/radio at very high spatial resolution, and locating the source of the weak non-thermal emission. We predict that the non-thermal emission occurs very close (a few milliarcseconds) to the OB component, where  $r_{OB}/D \sim 0.01$ .

It has been suggested by Dougherty *et al.* (2000) that some apparent discrepancies in the luminosities of the components in WR146 might be resolved if the O8 companion was itself a WR+O binary. Likewise, Setia Gunawan *et al.* (2000) have interpreted the observed 3.38 yr period in the 1.4 GHz radio emission as evidence for a third component in the system orbiting the O8 star. Our resolved spectra of WR146 shows no clear evidence for a third component. It is true that the CIV emission feature in the O8 star spectrum, which we marked as contaminated light from the WC6 star, does look significantly different from the actual CIV profile in the WC6

spectrum, and thus one may argue that the so-called "contaminated light" could actually be the signature of another WR star orbiting the O8 component. We note however that (1) the fact that the PSF is strongly dependent on the wavelength most likely introduces a dependency on wavelength for the amount of contaminated light which can distort the CIV profile on the O8 star, and (2) the extracted spectra being the result of a multidimensional fit of the whole double PSF profile, we do not necessarily expect the contamination to add up in a strictly linear fashion (i.e. effects may be non-linear), which means that a disproportionately strong contamination could occur at the point where the CIV line is brightest, hence distorting the CIV profile in the O8 star spectrum. We therefore conclude that there is no evidence for another WR star orbiting the O8 star component on a tighter orbit. We can safely rule out the presence of any unresolved WR star, except for one that would be significantly fainter (at least 1 magnitude) than the resolved WC6 component. Unless the WC6 is unusually bright for its spectral type, this leaves only a relatively faint WR star of spectral type WC3-WC4 or WN2-WN3 (see van der Hucht 2001) as a possible (but unlikely) candidate. If the O8 star is an unresolved double, it is more likely to be an OB+OB system.

## 5. Summary

We briefly summarize our findings as follows:

1. We have obtained resolved spectra of the components in the close visual binary systems WR86, WR146, and WR147. WR86 is classified as WC7+B0 III, with the WR component to the northwest and the B component to the southeast. WR146 is classified as WC6 + O8 I-IIf, with the WR component to the south and the O component to the north. WR147 is classified as WN8 + O5-7 I-II(f), with the WR component to the south and the O component to the north. The relative location of the WR and O components in the WR146 and WR147 systems is consistent with the colliding wind interpretation of their radio maps.
2. Absolute magnitudes  $M_V$  of the OB stars have been derived based on the spectral type-magnitude relationship of Schmidt-Kaler (1982), and compared with the estimated absolute magnitudes  $M_v$  of the Wolf-Rayet stars (from van der Hucht 2001). While the values are consistent for the WR86 system, we find a significant discrepancy in the WR146 and WR147 systems. For WR146, it looks like the WC6 star is at least 2 magnitudes brighter than expected (or the O8 I-IIf star is at least 2 magnitudes fainter than expected). For WR147 the WN8 star appears to be at least 1.5 magnitudes brighter than expected (or the O5-7 I-II(f) star is fainter than expected).
3. From the spectral types, we estimate that the O components in WR146 and WR147 have mass-loss rates  $\dot{M}_O \sim 10^{-5} M_\odot \text{ yr}^{-1}$ . These values can be compared to the estimated values for the WR component mass-loss rate  $\dot{M}_{WR}$ , which are linked to  $\dot{M}_O$  through the

configuration of the colliding-wind systems. While the estimated value of  $\dot{M}_O$  for WR146 is consistent with  $\dot{M}_{WR}$ , our value of  $\dot{M}_O$  for WR147 is an order of magnitude too large. This most likely indicates that our spectral classification is inaccurate, although it could also mean that current estimates of the distance to WR147 are too low. A more accurate spectral classification for WR147 is required to resolve the discrepancy, which will require new resolved spectroscopic observations of the OB component in WR147.

4. From the spectral type, we estimate the B component in WR86 to have  $\dot{M} \sim 10^{-7} M_{\odot} \text{ yr}^{-1}$ . The relatively smaller mass-loss rate in the OB component in WR86 must result in the colliding wind region being much smaller in volume and located much closer to the B star. Hence the amount of non-thermal emission arising in the shock cone is expected to be much smaller. The reduced mass-loss rate from the B star and smaller volume of the resulting shock cone explains why WR86 is found to be a weak non-thermal emitter, while WR146 and WR147 are known strong non-thermal emitters.
5. In none of the systems did we observe any trace of diffuse emission down to the instrumental limit. If there is any diffuse emission in the optical associated with the colliding wind interface, it must be weaker than  $5 \cdot 10^{-15} \text{ ergs cm}^{-2} \text{ s}^{-1} \text{ \AA}^{-1} \text{ arcsec}^{-1}$ .

Overall, we feel that the classification of OB stars, especially the determination of luminosity classes, is a difficult and non-trivial task. The main reason for this is the lack of availability of a uniform sequence of digital spectra spanning the whole spectral range from blue to red. Existing atlases, while useful, are sometimes fragmentary, and most are based on photographic spectra. Publication of a comprehensive atlas of digital spectra for OB stars based on CCD observations and covering the whole optical range from  $\sim 4000 - 7000 \text{ \AA}$  would be very beneficial to this field.

## REFERENCES

- Churchwell, E., Bieging, J. H., van der Hucht, K. A., Williams, P. M., Spoelstra, T. A. Th., & Abbott, D. C. 1992, *ApJ*, 393, 329
- Conti, P. S., & Alschuler, W. R. 1971, *ApJ*, 170, 325
- Conti, P. S. 1973, *ApJ*, 179, 181
- Conti, P. S. 1976, *Société Royale des Sciences de Liège, Mémoires*, vol. 9, 1976, p. 193-212
- Crowther, P., De Marco, O., Barlow, M. J. 1998, *MNRAS*, 296, 367
- Dougherty, S. M., Williams, P. M., van der Hucht, K. A., Bode, M. F., & Davis, R. J. 1996, *MNRAS*, 280, 963
- Dougherty, S. M. & Williams, P. M. 2000, *MNRAS*, 319, 1005



- Dougherty, S. M., Williams, P. M., & Pollacco, D. L. 2000, MNRAS, 316, 143
- Eenens, P. R. J., & Williams, P. M. 1994, MNRAS, 269, 1082
- Eichler, D., & Usov, V. 1993, ApJ, 402, 271
- Hartkopf, W. I., Mason, B. D., Barry, D. J., McAlister, H. A., Bagnuolo, W. G., & Prietro, C. M. 1993, AJ, 106, 352-360
- Herrero, A., Puls, J., & Villamariz, M. R. 2000, A&A, 354, 193
- Jeffers, H. M., van de Bos, W. H., & Greeby, F. M. 1963, *Index Catalog of Visual Double Stars, 1961.0*, Publ. Lick Obs. 21, part 1
- Lundstrom, I., & Stenholm, B. 1984, A&AS, 58, 163
- Milward, C. G., & Walker, G. A. H. 1985, ApJS, 57, 63
- Massey, P., Conti, P. S., Niemela, V. S. 1981, ApJ, 246, 145
- Moffat, A. F. J. 1969, A&A, 3, 455
- Moffat, A. F. J. 1995, IAU Symp. 163, Properties of Wolf-Rayet Binaries: The Key to Understanding Wolf-Rayet Stars (Dordrecht: Kluwer), 213
- Moffat, A. F. J., Lamontagne, R., Shara, M. M., McAlister, H. A. 1986, AJ, 91, 1392-1399
- Niemela, V. S., Shara, M. M., Wallace, D. J., Zurek, D. R., Moffat, A. F. J. 1998, AJ, 115, 2047
- Prinja, R. K., Barlow, M. J., & Howarth, I. D. 1990, ApJ, 361, 607
- Roberts, M. S., 1962, AJ, 67, 79-85
- Runacres, M. C., & Blomme, R. 1996, A&A, 309, 544
- Schmidt-Kaler, T. 1982, Numerical Data Functional Relationships in Science & Technology, Landoldt-Bornstein, New Series, Group 6, Vol. 2b, ed. K. Schaiffers & H.H. Voigt, (Berlin: Springer), p.1
- Setia Gunawan, D. Y. A., van der Hucht, K. A., de Bruyn, A. G., & Williams, P. M. 2000, A&A, 356, 676
- Smith, L. F. 1968, MNRAS, 138, 109-121
- Smith, L. F., Shara, M. M., Moffat, A. F. J. 1990, ApJ, 358, 229
- Smith, L. F., Shara, M. M., Moffat, A. F. J. 1996, MNRAS, 281, 163

- Turner, D. G. 1982, In: Wolf-Rayet stars: Observations, physics, evolution; Proceedings of the Symposium, Cozumel, Mexico, September 18-22, 1981. (A82-48127 24-90) Dordrecht, D. Reidel Publishing Co., p. 57-60
- Tuthill, P. G., Monnier, J. D., Danchi, W. C. *Nature*, 398, 487
- van der Hucht 1992, *Astronomy and Astrophysics Review*, vol. 4, no. 2, p. 123
- van der Hucht, K. A. 2001, *New Astronomy Reviews*, 45, 135
- van der Hucht, K. A., Conti, P. S., Lundstrom, I., & Stenholm, B. 1981, *Space Sci. Rev.*, 28, 227
- Walborn, N. R. 1980, *ApJS*, 44 535
- Walborn, N. R., Fitzpatrick, E. L. 1990, *PASP*, 102, 379
- Wallace, D. J., Gies, D. R., Nelan, E., & Leitherer, C. 2000, *BAAS*, Volume 32, No. 4, #97.04
- Wegner, W. 2000, *MNRAS*, 319, 771
- Westerlund, B. E. 1966, *ApJ*, 145, 724
- Williams, P. M., Radio emission from the stars and the sun. ASP Conference Series, Volume 93; Proceedings of a conference held at the University of Barcelona; Barcelona; Spain; 3-7 July 1995, edited by A. R. Taylor and J. M. Paredes, p.15
- Williams, P. M., Dougherty, S. M., Davis, R. J., van der Hucht, K. A., Bode, M. F., Setia Gunawan, D. Y. 1997, *MNRAS*, 289, 10
- Williams, P. M., 1999, “Proceedings of the 193rd symposium of the International Astronomical Union held in Puerto Vallarta, Mexico, 3-7 November 1998”. Edited by K. A. van der Hucht, G. Koenigsberger, and P. R. J. Eenens. San Francisco, Calif. : Astronomical Society of the Pacific, 1999., p.267

Table 1. Line identifications in the spectrum of the WR component of WR86

ID	$\lambda_{lab}(\text{\AA})$	$W_{\lambda}(\text{\AA})$
HeII	4338.7	-25.0±5.0
CIV	4441.5	-31.9±0.5
HeII	4541.6	-15.0±5.0
OIII/OV	5592.2/5597.9	-31.8±2.0
CIII	5695.9	-205.±15.
CIV	5801.3/5812.0	-295.±15.
HeI	5875.6	-50.0±5.0
HeII	6406.4	-13.0±3.0
HeII	6560.0	-85.0±10.
CIII	6744.4	-120.±10.

Table 2. Line identifications in the spectrum of the OB component of WR86

ID	$\lambda_{lab}(\text{\AA})$	$\lambda_{obs}(\text{\AA})$	$W_{\lambda}(\text{\AA})$
H $_{\gamma}$	4340.5	4341.7	2.30±0.20
OII	4349.4	4349.0	0.70±0.20
HeI	4387.9	4389.2	0.55±0.05
OII	4414.9	4417.3	0.35±0.05
OII	4448.3	4449.3	0.20±0.05
HeI	4471.5	4472.4	1.00±0.10
MgIII	4479.0	4482.1	0.15±0.05
NII	4530.4	4530.7	0.15±0.05
SiIII	4553.9	4554.2	0.35±0.05
SiIII	4567.8	4569.1	0.30±0.05
SiIII	5739.7	5741.6	0.30±0.05
HeI	5875.6	5877.2	0.70±0.05
H $_{\alpha}$	6561.9	6564.8	2.00±0.05
HeI/HeII	6678.1/6683.2	6679.8	0.80±0.05

Table 3. Line identifications in the spectrum of the WR component of WR146

ID	$\lambda_{lab}(\text{\AA})$	$W_{\lambda}(\text{\AA})$
OIII/OV	5592.2/5597.9	-22.0±3.0
CIII	5695.9	-55.0±8.0
CIV	5801.3/5812.0	-600.±35.
HeI	5875.6	-140.±35.
HeII	6406.4	-15.0±3.0
HeII	6560.0	-165.±10.
CIII	6744.4	-200.±15.

Table 4. Line identifications in the spectrum of the OB component of WR146

ID	$\lambda_{lab}(\text{\AA})$	$\lambda_{obs}(\text{\AA})$	$W_{\lambda}(\text{\AA})$
H $_{\gamma}$	4340.5	4339.6	1.50±0.10
HeI	4387.9	4388.7	0.20±0.05
HeI	4471.5	4470.0	0.80±0.05
HeII	4541.5	4540.3	0.40±0.05
CIII	5695.9	5695.1	-0.65±0.05
CIV	5811.9	5811.2	0.22±0.05
HeI	5875.6	5874.8	1.0±0.10
H $_{\alpha}$	6561.9	6568.3	-4.85±0.25
HeI/HeII	6678.1/6683.2	6678.3	0.15±0.05

Table 5. Line identifications in the spectrum of the WR component of WR147

ID	$\lambda_{lab}(\text{\AA})$	$W_\lambda(\text{\AA})$
NII	5679.6	$-6.0 \pm 1.0$
NIV	5736.9	$-5.8 \pm 1.0$
CIV	5801.3/5812.0	$-0.8 \pm 0.2$
HeI	5875.6	$-35.0 \pm 1.0$
HeII	6310.8	$-0.6 \pm 0.2$
NIV	6380.7	$-0.8 \pm 0.2$
HeII	6406.4	$-0.9 \pm 0.2$
NIII	6467.0/6478.7	$-3.2 \pm 0.3$
HeII	6527.1	$-1.0 \pm 0.1$
HeII	6560.0	$-45.0 \pm 1.5$
HeI/HeII	6678.1/6683.2	$-30.0 \pm 1.5$

Table 6. Line identifications in the spectrum of the OB component of WR147

ID	$\lambda_{lab}(\text{\AA})$	$\lambda_{obs}(\text{\AA})$	$W_\lambda(\text{\AA})$
CIV	5801.3	5802.5	$0.40 \pm 0.10$
CIV	5811.9	5812.5	$0.35 \pm 0.10$
HeI	5875.6	5875.9	$0.45 \pm 0.10$
H $_\alpha$	6561.9	6570.8	$-4.05 \pm 0.05$

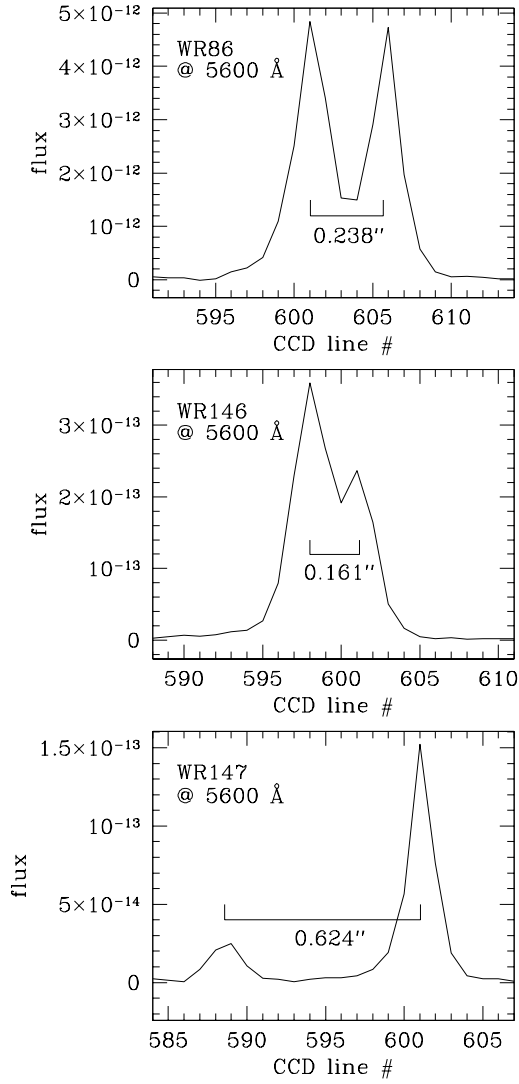


Fig. 1.— Resolution of the WR+O systems along the slit of the STIS camera at 5600 Å. The slit is oriented along the line joining the stars, with the OB star to the left and the WR star to the right on this figure.

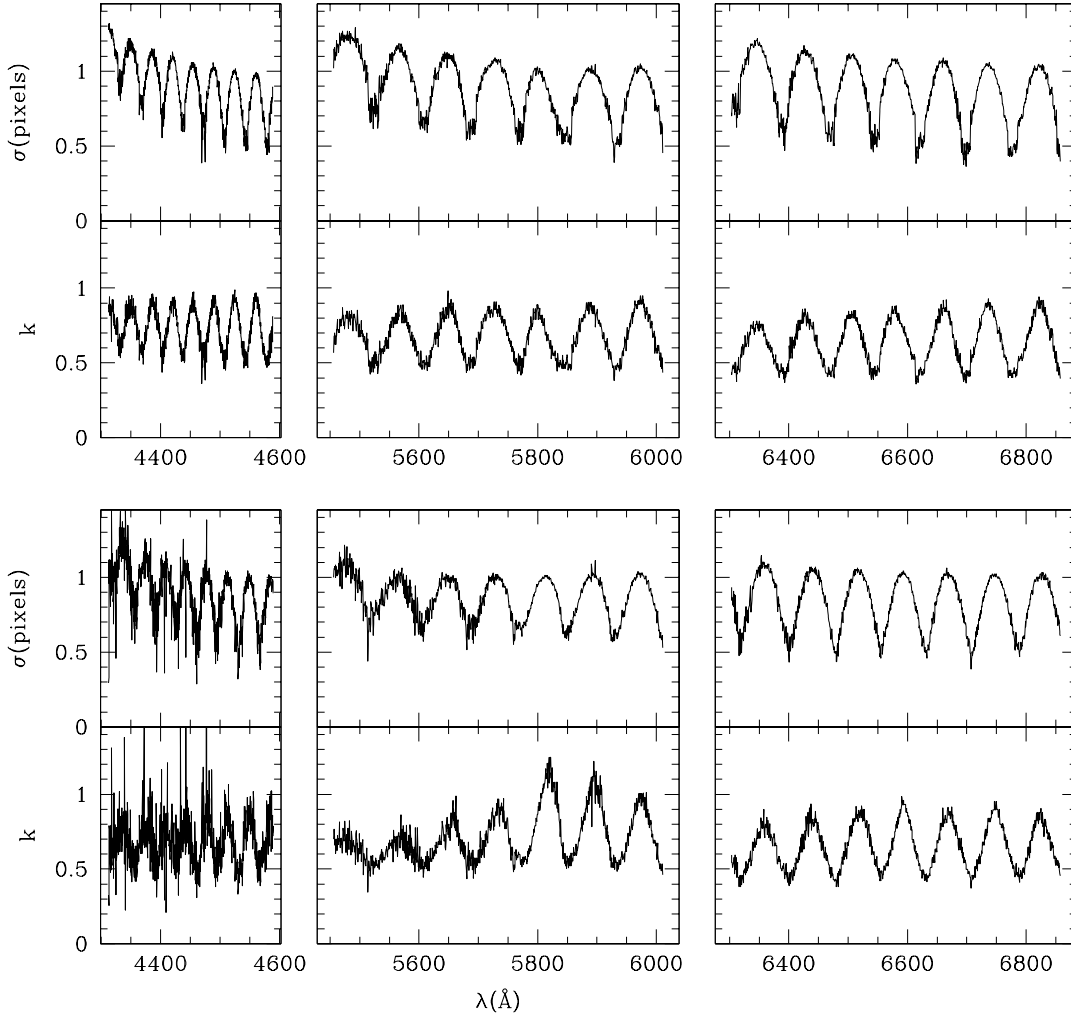


Fig. 2.— Dispersion parameter  $\sigma$  and “peakyness” parameter  $k$  of the stellar profiles measured for the WR86 (top) and WR146 (bottom) systems. Values are derived from a double-profile multidimensional fit at each column on the STIS CCD image. The point spread function is clearly dependent on the wavelength; patterns also differ significantly between systems. The fit also yields deblended spectra of the individual components (Figures 3-6). Deblending is reasonably good, except at wavelengths where the WR star becomes  $\gtrsim 3$  times brighter than the O star, at which point this model is not accurate enough to yield reliable deblended spectra (see text).

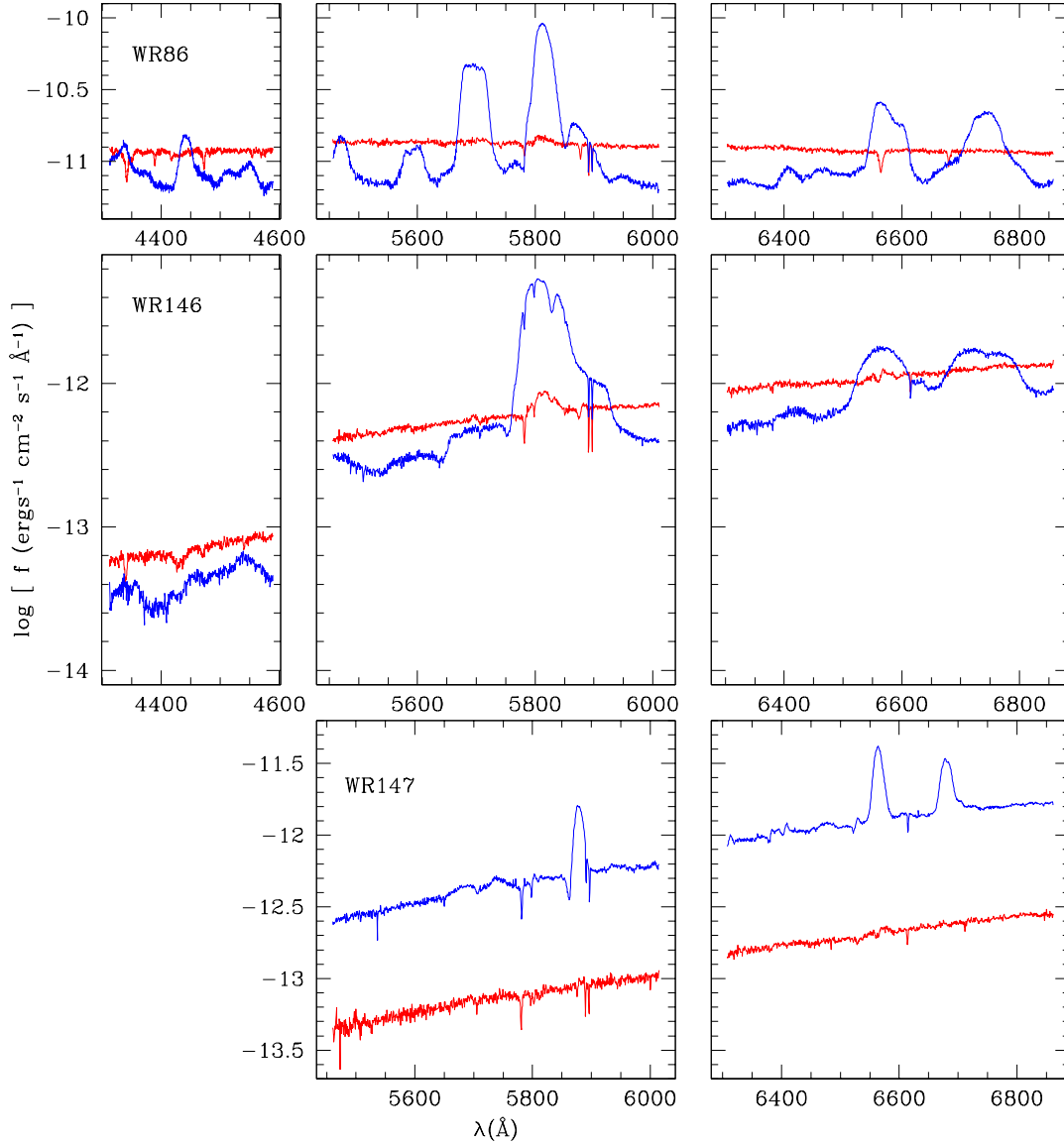


Fig. 3.— Resolved STIS spectra of the WR86, WR146, and WR147 systems (from top to bottom, respectively). Contamination of the OB spectrum by the brightest of the WR star features occurred in WR86 and in WR146 (CIV  $\lambda 5812$  emission line) because the stars were only separated by  $\approx 2$  standard deviations of the STIS point spread function. Note the similar amounts of reddening and equivalent strengths of the interstellar absorption features for the pairs of stars in each system. Line identification is provided in Figures 4-9.



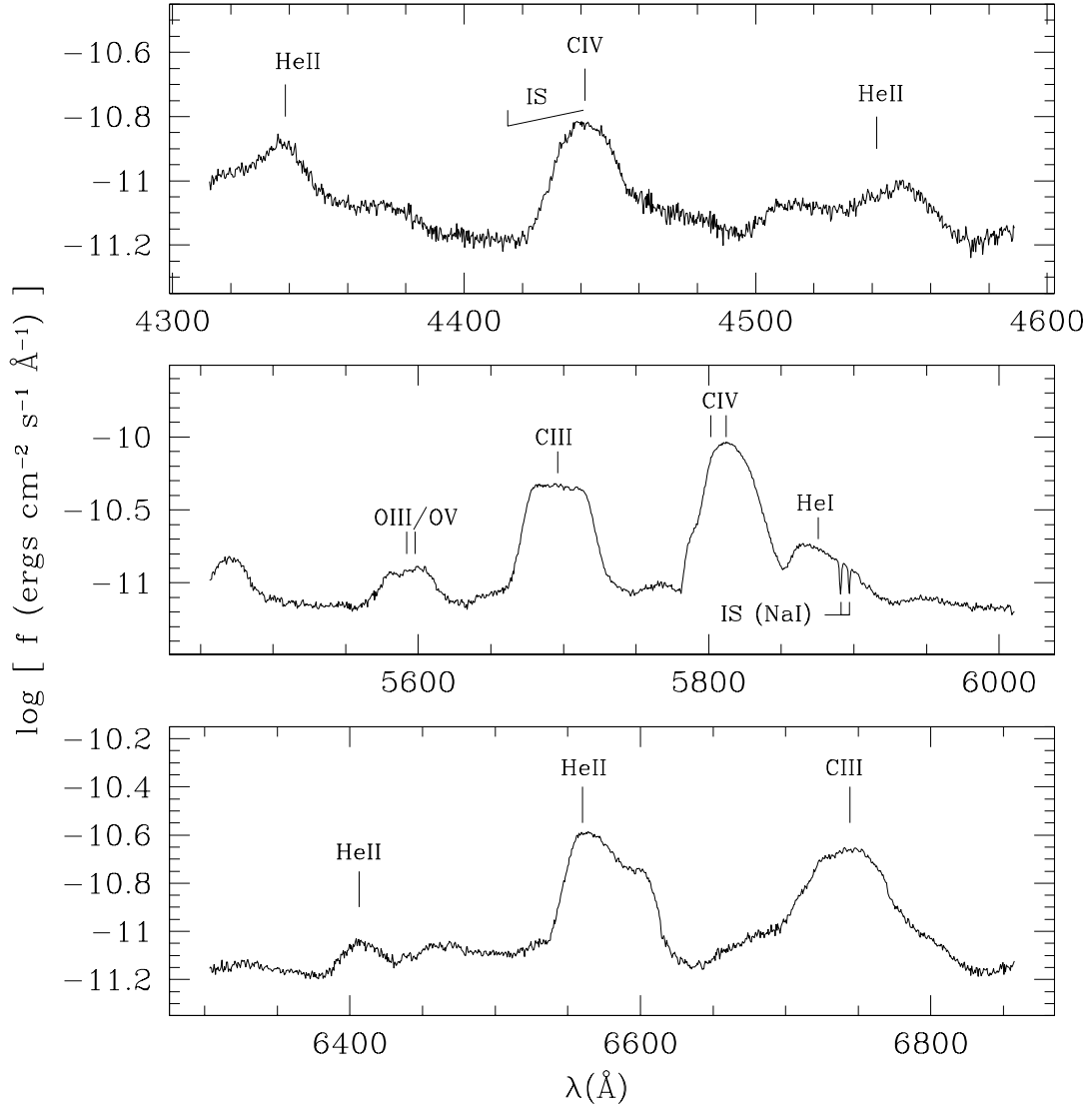


Fig. 4.— Line identification for the WR star component in the WR86 system. Because emission-lines are very broad, most of the features identified here are actually blends of several different lines. The identification is for the main contributor to each feature. Equivalent widths are listed in Table 1.

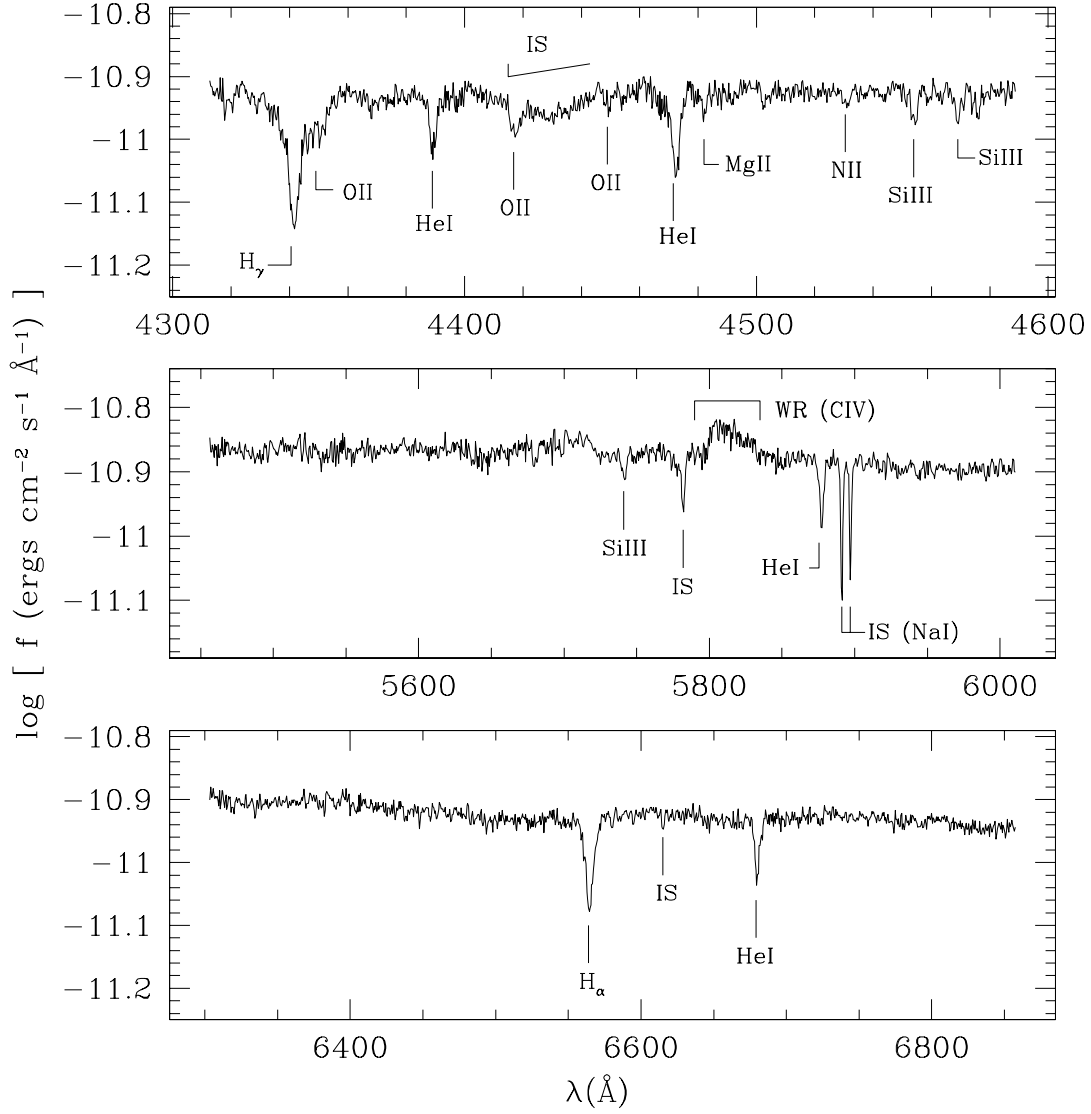


Fig. 5.— Line identification for the B star component in the WR86 system. Contamination from the WR star is noted, along with the principal interstellar absorption features. Equivalent widths are listed in Table 2. The feature noted WR(CIV) is an instrumental contamination of the light from the WR component.

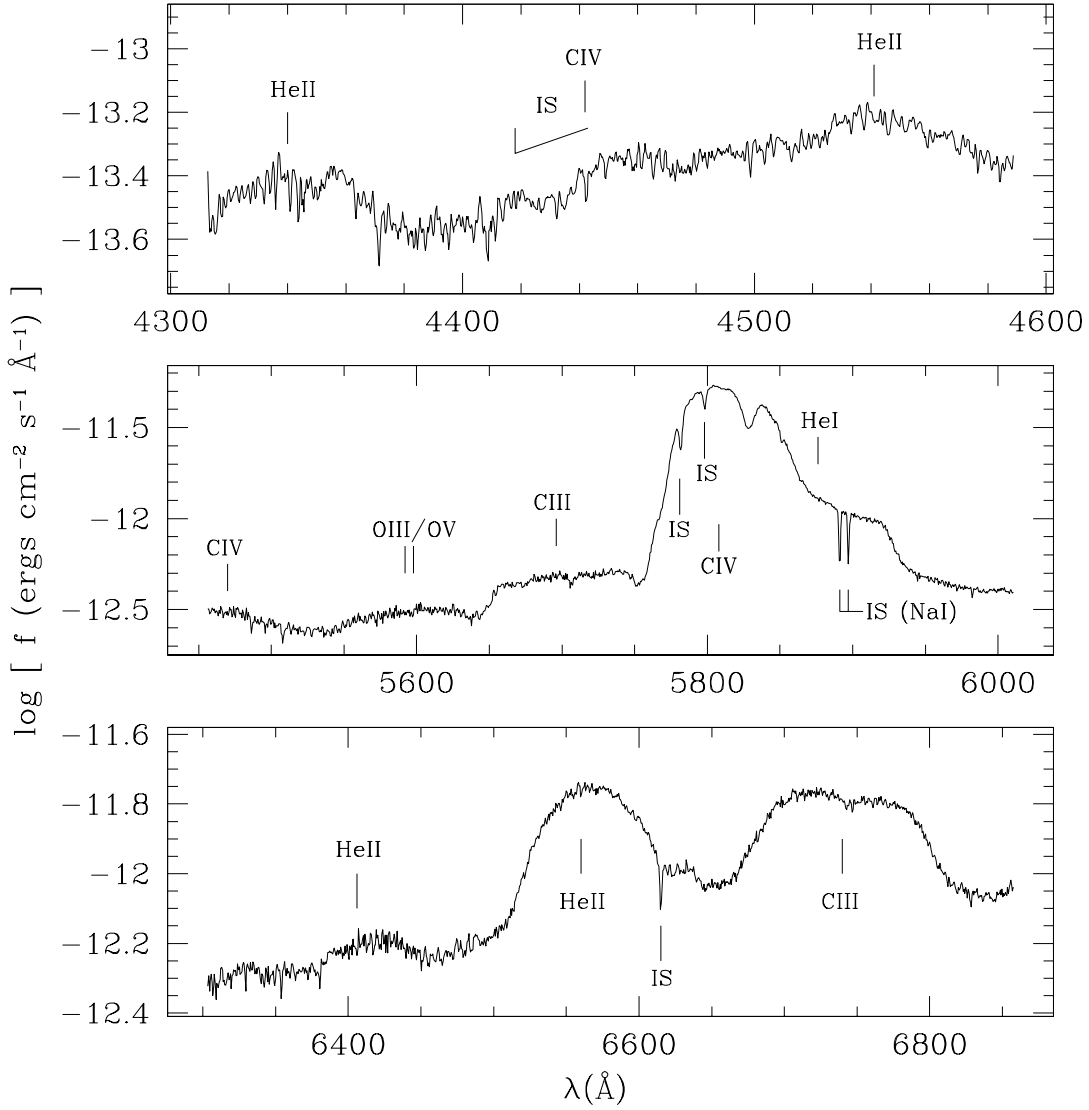


Fig. 6.— Line identification for the WR star component in the WR146 system. Because emission-lines are very broad, most of the features identified here are actually blends of several different lines. The identification is for the main contributor to each feature. Equivalent widths are listed in Table 3.

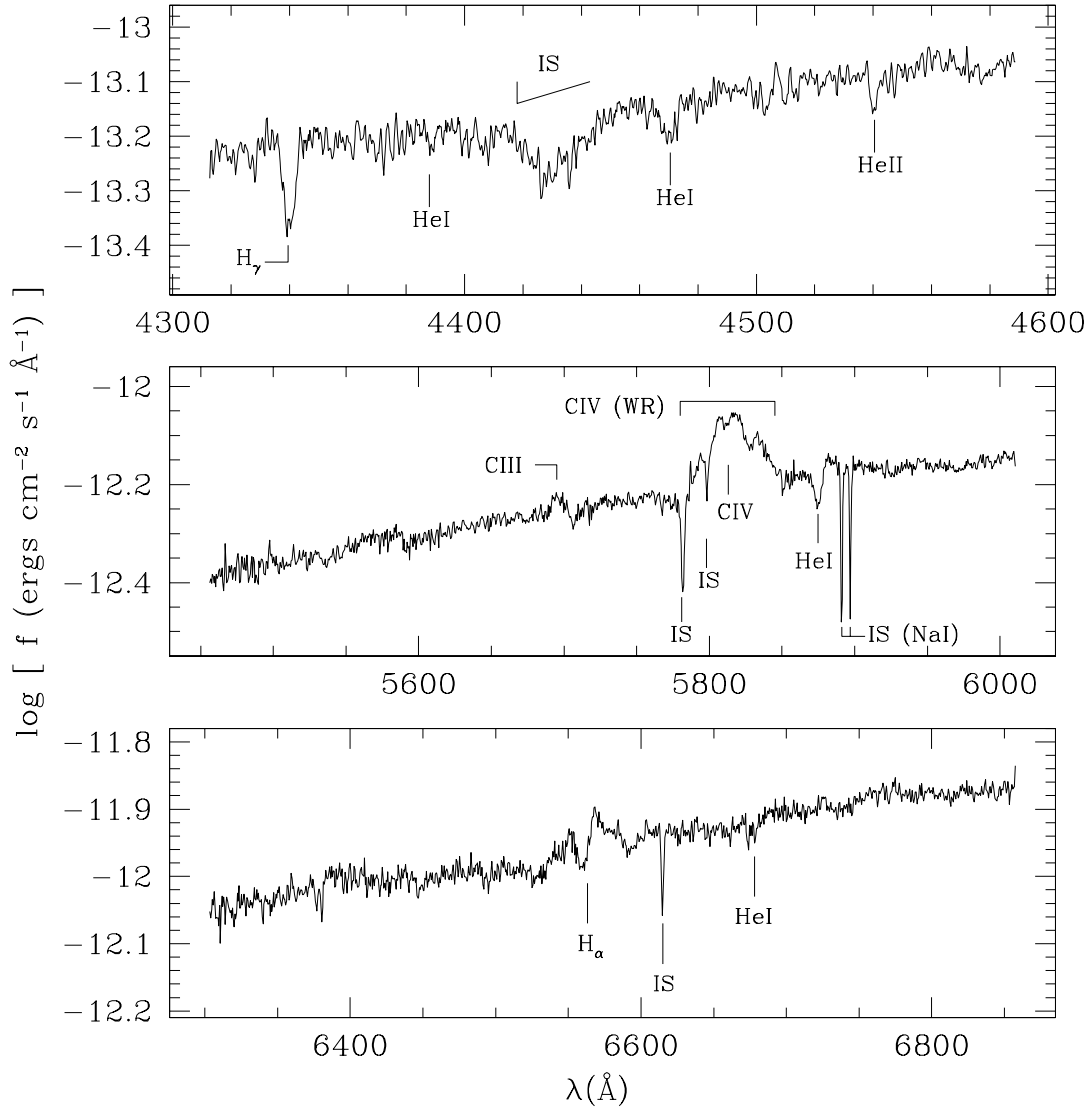


Fig. 7.— Line identification for the O star component in the WR146 system. Contamination from the WR star is noted, along with the principal interstellar absorption features. Equivalent widths are listed in Table 4. The feature noted CIV(WR) is an instrumental contamination of the light from the WR component.

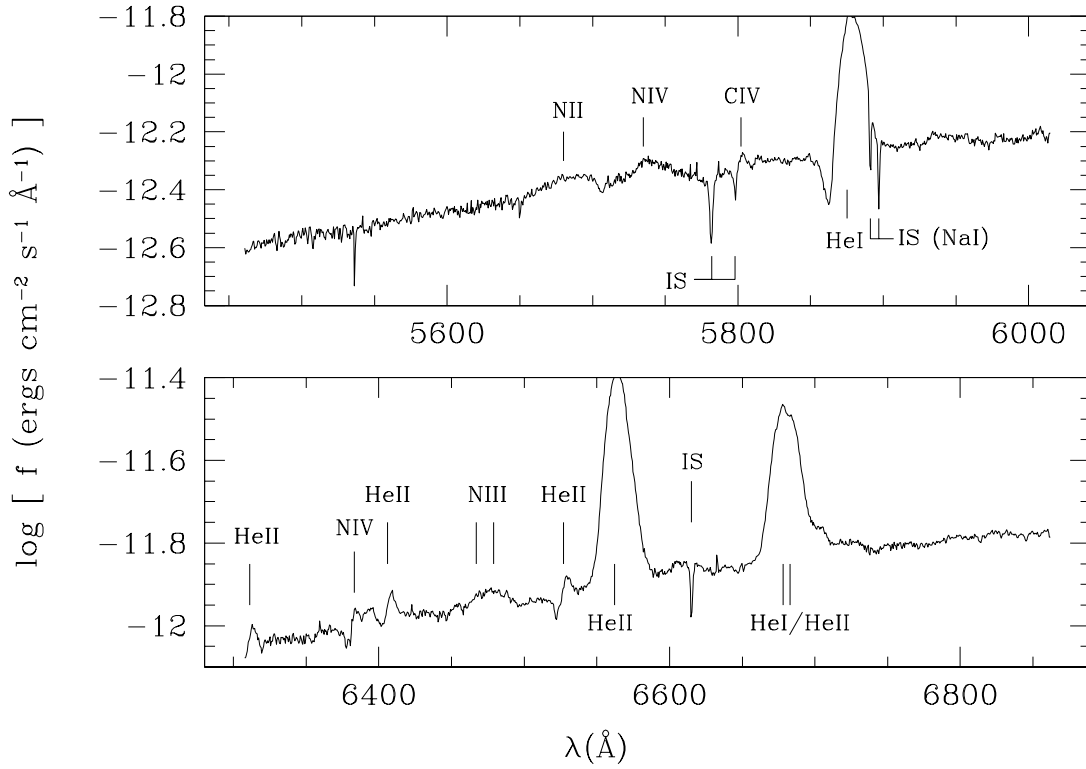


Fig. 8.— Line identification for the WR star component in the WR147 system. Because emission-lines are very broad, most of the features identified here are actually blends of several different lines. The identification is for the main contributor to each feature. Equivalent widths are listed in Table 5.

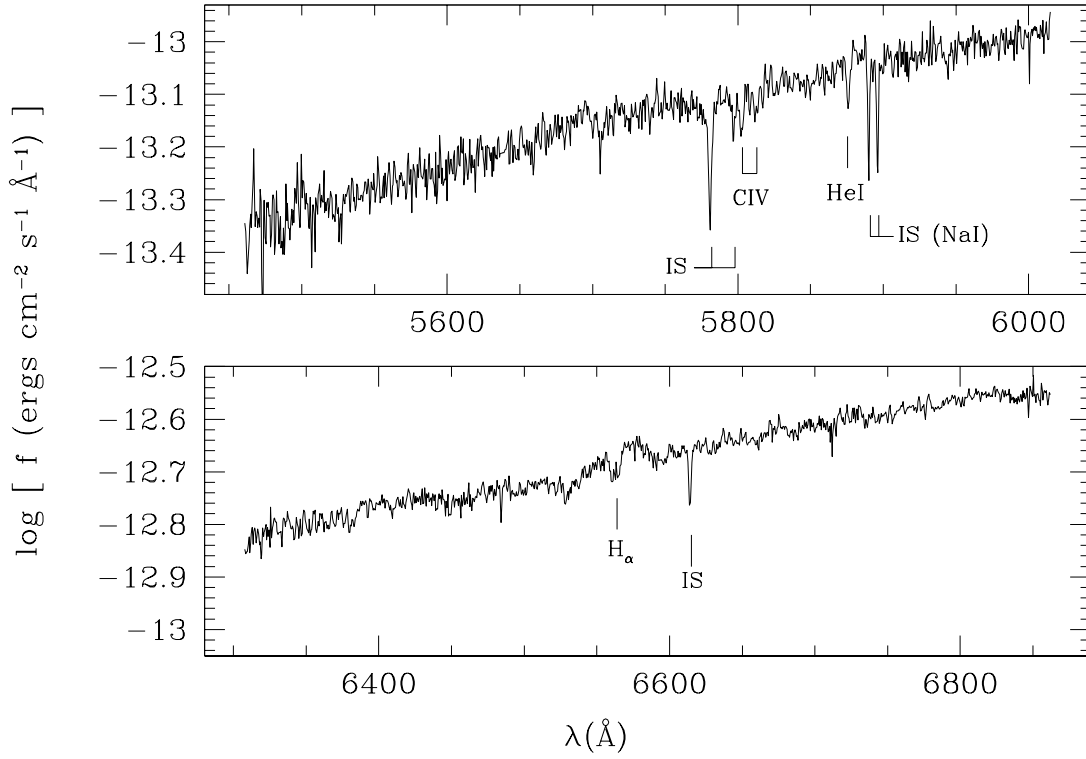


Fig. 9.— Line identification for the O star component in the WR147 system. Well-defined intrinsic and interstellar absorption features are noted. Equivalent widths are listed in Table 6.